



www.sciencemag.org/cgi/content/full/334/6056/629/DC1

Supporting Online Material for

Porphyrin-Sensitized Solar Cells with Cobalt (II/III)–Based Redox Electrolyte Exceed 12 Percent Efficiency

Aswani Yella, Hsuan-Wei Lee, Hoi Nok Tsao, Chenyi Yi, Aravind Kumar Chandiran, Md.Khaja Nazeeruddin, Eric Wei-Guang Diao,* Chen-Yu Yeh,* Shaik M. Zakeeruddin,* Michael Grätzel*

*To whom correspondence should be addressed. E-mail: michael.gratzel@epfl.ch (M.G.); shaik.zakeer@epfl.ch (S.M.Z.); diao@mail.nctu.edu.tw (E.W.-G.D.); cyyeh@dragon.nchu.edu.tw (C.-Y.Y.)

Published 4 November 2011, *Science* **334**, 629 (2011)
DOI: 10.1126/science.1209688

This PDF file includes:

Materials and Methods

Figs. S1 to S12

Tables S1 to S4

References (47, 48)

Supporting Online Material for

Porphyrin-Sensitized Solar Cells with Cobalt (II/III) Based Redox Electrolyte

Exceed 12% Efficiency

Aswani Yella,^a Hsuan-Wei Lee,^b Hoi Nok Tsao,^a Chenyi Yi,^a Aravind Kumar Chandiran,^a Md.Khaja Nazeeruddin^a, Eric Wei-Guang Diao,^c Chen-Yu Yeh,^b Shaik M Zakeeruddin,^a Michael Grätzel.^a

General

All reagents and solvents were obtained from commercial sources and used without further purification unless otherwise noted. CH₂Cl₂ was dried over CaH₂ and freshly distilled before use. THF was dried over sodium/ benzophenone and freshly distilled before use. Tetra-*n*-butylammonium hexafluorophosphate (TBAPF₆) was recrystallized twice from absolute ethanol and further dried for two days under vacuum. Column chromatography was performed on silica gel (Merck, 70-230 Mesh ASTM).

Device Fabrication

The photoanode used in this study consists of thin TiO₂ electrodes comprising a 5 μm mesoporous TiO₂ layer (particle size, 20 nm, pore size 32 nm) and a 5 μm TiO₂ scattering layer (particle size, 400 nm). Thickness and the porosity of the photoanode was found to be very crucial in the cobalt based DSSCs. Porosity of the TiO₂ paste was increased (from 23 nm pore size to 32 nm pore size) and the thickness

^a Laboratory for Photonics and Interfaces, Institute of Chemical Sciences and Engineering, École Polytechnique Fédérale de Lausanne, Lausanne-1015, Switzerland. E-mail: shaik.zakeer@epfl.ch, michael.graetzel@epfl.ch

^b Department of Chemistry and Center of Nanoscience & Nanotechnology, National Chung Hsing University, Taichung, Taiwan 402, ROC. E-mail: cyyeh@dragon.nchu.edu.tw

^c Department of Applied Chemistry **and Institute of Molecular Science**, National Chiao Tung University, Hsinchu, Taiwan 300, ROC. E-mail: diao@mail.nctu.edu.tw

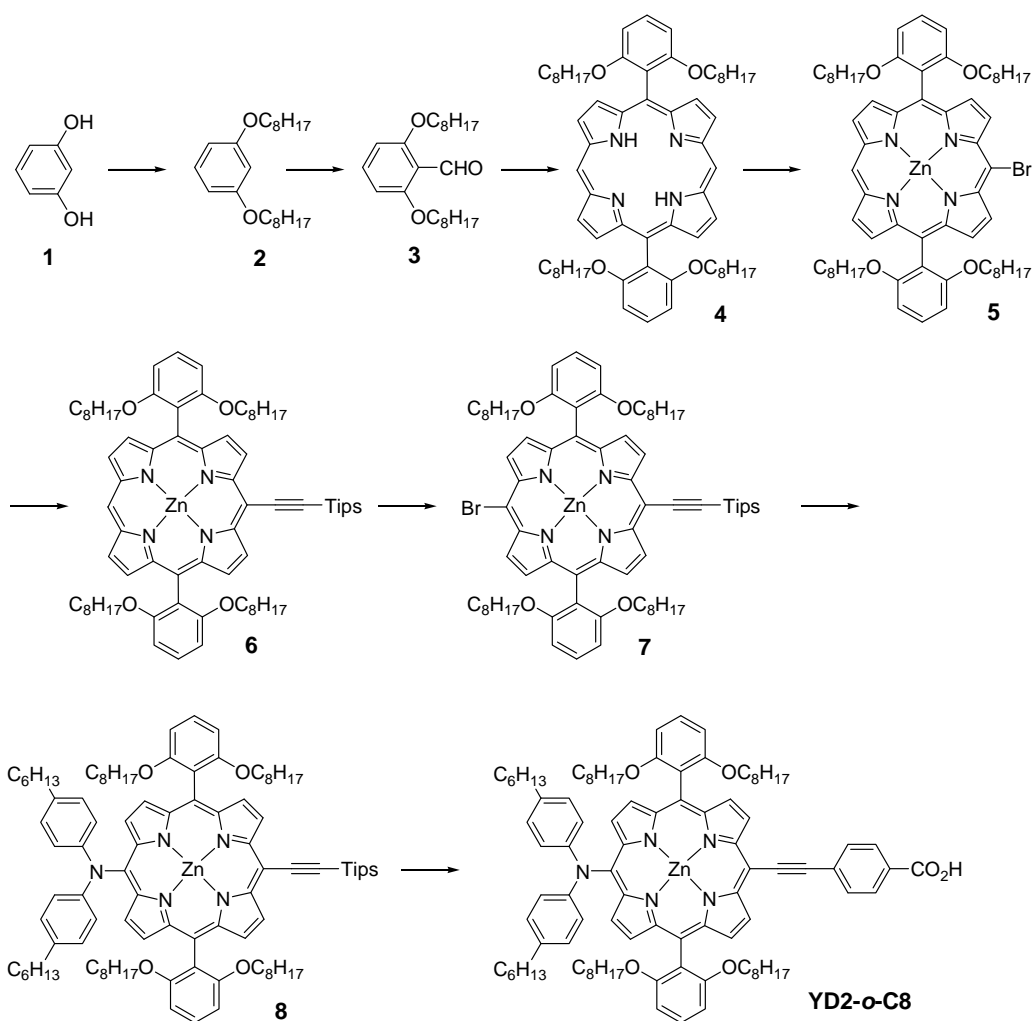
was reduced compared to I⁻/I₃⁻ based devices to avoid the mass transport limitations in

cobalt based devices. Both the porphyrin dyes **YD2** and **YD2-*o*-C8** were tested as photosensitizers for DSC devices. The working electrode was prepared by immersing the 10 μm (5 μm thick transparent layer +5 μm thick scattering layer) TiO_2 film into dye solution for 18 h. A thermally platinized FTO glass counter electrode and the working electrode were then sealed with a 25 μm thick hot-melt film (Surlyn, by heating the system at 100°C. Devices were completed by filling the electrolyte by pre-drilled holes in the counter electrodes and finally the holes were sealed with a Surlyn sheet and a thin glass cover by heating. A black mask (6x6 mm^2) was used in subsequent photovoltaic studies.

Spectral and Electrochemical Measurements

^1H NMR spectra (Varian spectrometer) at 400 MHz, UV-visible spectra (Varian Cary 50), emission spectra (a JASCO FP-6000 spectrofluorometer), FAB-MS mass spectra (Bruker APEX II spectrometer, operating in the positive ion detection mode) were recorded on the indicated instruments. Electrochemical tests were performed with a three-electrode potentiostat (CH Instruments, Model 750A) in THF deoxygenated on purging with pre-purified dinitrogen gas. Cyclic voltammetry experiments for porphyrin dyes was conducted with a three-electrode cell equipped with a BAS glassy carbon (0.07 cm^2) disk as the working electrode, a platinum wire as the auxiliary electrode, and a Ag/AgCl (saturated) reference electrode. The reference electrode is separated from the bulk solution by a double junction filled with electrolyte solution. Potentials are reported vs. Ag/AgCl (saturated) with reference to a ferrocene/ferrocenium (Fc/Fc^+) couple at $E_{1/2} = +0.63$ vs Ag/AgCl (saturated) at 23 °C in THF. The working electrode was polished with 0.03 μm aluminium on felt pads (Buehler) and treated ultrasonically for 1 min before each experiment. The reproducibility of individual potential values was within ± 5 mV. Cyclic Voltammetry experiments for the cobalt complex employed 1mM $[\text{Co}(\text{bpy})_3](\text{B}(\text{CN})_4)_2$ and 0.1 M tetra-butylammonium hexafluorophosphate in acetonitrile and a Ag/Ag $^+$ electrode as a reference in the same solvent, containing 0.1 M AgNO_3 and 0.1 M tetrabutylammonium hexafluorophosphate electrolyte. The latter was calibrated with respect to the ferrocene/ferricenium redox couple using $E^\circ (\text{Fc}/\text{Fc}^+) = +0.63$ vs NHE.

Synthetic Route to **YD2-*o*-C8**:



1,3-Dioctoxybenzene (2)

Compound **2** was prepared under modified conditions of literature procedure. (47) A mixture of resorcinol (11 g, 0.1 mol), 1-bromooctane (69.6 mL, 0.4 mol) and K_2CO_3 (69 g, 0.5 mol) was refluxed for 4 days in dry acetone (500 mL). The solvent was removed under reduced pressure and extracted with EtOAc (3×100 mL). The combined extracts were washed with water and dried over anhydrous $MgSO_4$. After removal of solvent under reduced pressure, the product was purified by column chromatography eluting with hexanes to give 1,3-di(octyloxy)benzene (26.5 g, 79%). 1H NMR ($CDCl_3$, 400 MHz) δ_H 7.15 (t, $J=8.4$ Hz, 1H), 6.47 (m, 3H), 3.92 (t, $J=6.4$ Hz, 4H), 1.76 (m, 4H), 1.44 (m, 4H), 1.32-1.28 (m, 16H), 0.88 (t, $J=7.6$ Hz, 6H).

2,6-Dioctoxybenzaldehyde (3)

Compound **3** was prepared under modified conditions of literature procedure. (48) A

three-neck flask was equipped with an addition funnel and charged with compound **1** (10 g, 0.03 mol) and tetramethylethylenediamine (TMEDA) (1.15 mL) in 84 mL of tetrahydrofuran. The solution was degassed with dinitrogen for 15 min and cooled to °C, and then *n*-butyllithium (22.4 mL, 1.6 M solution in hexanes 0.036 mol) was dropwise over 20 min and allowed to stir for 3 h. After warming to room temperature, dimethylformamide (DMF) (4.38 mL, 0.06 mol) was added dropwise, and the mixture was stirred for an additional 2 h. The reaction was quenched with water, and the mixture was extracted with ether (3 × 80 mL), dried over anhydrous MgSO₄, and the solvent was removed under reduced pressure. The product was recrystallized from hexanes to yield a white solid (8.67 g, 80% yield). ¹H NMR (CDCl₃, 400 MHz) δ_H 10.54 (s, 1H), 7.38 (t, *J*=8.4 Hz, 1H), 6.53 (d, *J*=8.4 Hz, 2H), 4.02 (t, *J*=6.4 Hz, 4H), 1.86-1.79 (m, 4H), 1.58-1.42 (m, 4H), 1.38-1.25 (m, 16H), 0.88 (t, *J*=7.2 Hz, 6H). ¹³C NMR (CDCl₃, 100 MHz) δ_C 189.4, 162.0, 135.8, 115.1, 104.9, 69.2, 32.1, 29.6, 29.5, 29.4, 26.3, 23.0, 14.4. FAB-MS: *m/z* calcd for C₂₃H₃₈O₃ 362, found 362 [M]⁺.

5,15-Bis(2,6-dioctoxyphenyl)porphyrin (4)

To a degassed solution of dipyrromethane (6.04 g, 41.4 mmol) and compound **3** (15 g, 41.4 mmol) in DCM (5.4 L) was added trifluoroacetic acid (2.75 mL, 37.3 mmol). After the solution was stirred at 23 °C under dinitrogen for 4 h, DDQ (14.1 g, 62.1 mmol) was added and the mixture was stirred for an additional 1 h. The mixture was basified with Et₃N (7 mL) and filtered through silica. The solvent was removed under reduced pressure and the residue was purified by column chromatography (silica gel) using DCM/hexanes = 1/2 as eluent. The product was recrystallized from MeOH/CH₂Cl₂ to give the product (6.25 g, 30.7%) as a purple powder. ¹H NMR (CDCl₃, 400 MHz) δ_H 10.15 (s, 2H), 9.26 (d, *J*=4.8 Hz, 4H), 8.98 (d, *J*=4.8 Hz, 4H), 7.71 (t, *J*=8.4 Hz, 2H), 7.02 (d, *J*=8.4 Hz, 4H), 3.83 (t, *J*=6.4 Hz, 8H), 0.95-0.88 (m, 8H), 0.87-0.82 (m, 8H), 0.68-0.61 (m, 8H), 0.59-0.54 (m, 28H), 0.49-0.42 (m, 8H), -3.02 (s, 2H). ¹³C NMR (CDCl₃, 100 MHz) δ_C 160.7, 148.2, 145.5, 131.3, 130.9, 130.5, 120.6, 112.0, 105.9, 104.4, 69.2, 31.8, 29.1, 25.8, 22.8, 14.3. FAB-MS: *m/z* calcd for C₆₄H₈₆N₄O₄ 974, found 975 [M+1]⁺.

5-Bromo-10,20-bis(2,6-dioctoxyphenyl)porphyrin

To a stirred solution of porphyrin **4** (3.5 g, 3.59 mmol) in DCM (1500 mL) was slowly added a solution of NBS (0.671g, 3.77 mmol) in DCM (400 mL) in a period of 6 h at 0 °C under dinitrogen. After the reaction was quenched with acetone (30 mL), the solvent was removed under reduced pressure. The residue was purified by column

chromatography (silica gel) using DCM/hexanes = 1/2 as eluent. Recrystallization from MeOH/DCM gave the product (2.3 g, 61%) as a purple powder. ¹H NMR (CDCl₃, 400 MHz) δ_H 10.01 (s, 1H), 9.62 (d, *J*=4.8 Hz, 2H), 9.17 (d, *J*=4.4 Hz, 2H), 8.88 (t, *J*=4.8 Hz, 4H), 7.70 (t, *J*=8.0 Hz, 2H), 7.01 (d, *J*=8.4 Hz, 4H), 3.84 (t, *J*=6.4 Hz, 8H), 0.97-0.90 (m, 8H), 0.86-0.79 (m, 8H), 0.67-0.60 (m, 8H), 0.58-0.49 (m, 28H), 0.47-0.39 (m, 8H), -2.89 (s, 2H). ¹³C NMR (CDCl₃, 100 MHz) δ_C 160.5, 132.3, 131.8, 130.6, 120.4, 113.3, 105.6, 104.7, 102.6, 69.1, 31.8, 29.1, 29.0, 25.8, 25.7, 22.7, 14.3. FAB-MS: *m/z* calcd for C₆₄H₈₅BrN₄O₄ 1054, found 1054 [M]⁺.

[5-Bromo-10,20-bis(2,6-di-octoxyphenyl)porphinato] zinc(II) (5)

A suspension of 5-Bromo-10,20-bis(2,6-dioctoxyphenyl)porphyrin (2.3 g, 2.18 mmol) and Zn(OAc)₂•2H₂O (4.79 g, 21.82 mmol) in a mixture of DCM (450 mL) and MeOH (220 mL) was stirred at 23 °C for 3 h. The reaction was quenched with water (100 mL), and the mixture was extracted with DCM (2 × 100 mL). The combined extracts were washed with water and dried over anhydrous MgSO₄. The solvent was removed under reduce pressure to give the product (2.39 g, 98%). ¹H NMR (CDCl₃, 400 MHz) δ_H 10.17 (s, 1H), 9.80 (d, *J*=4.8 Hz, 2H), 9.34 (d, *J*=4.8 Hz, 2H), 9.07 (t, *J*=4.8 Hz, 4H), 7.76 (t, *J*=8.0 Hz, 2H), 7.07 (d, *J*=8.4 Hz, 4H), 3.91 (t, *J*=6.4 Hz, 8H), 1.03-0.97 (m, 8H), 0.88-0.80 (m, 8H), 0.66-0.40 (m, 44H). ¹³C NMR (CDCl₃, 100 MHz) δ_C 160.5, 151.5, 151.4, 150.4, 149.3, 132.9, 132.8, 132.7, 132.6, 132.5, 132.1, 130.3, 121.5, 114.1, 105.8, 104.1, 69.1, 31.7, 29.1, 29.0, 25.7, 22.7, 14.3. FAB-MS: *m/z* calcd for C₆₄H₈₃BrN₄O₄Zn 1116, found 1116 [M]⁺.

[5,15-Bis(2,6-di-octoxyphenyl)-10-(triisopropylsilyl)ethynyl-porphinato] zinc(II) (6)

A mixture of the zinc complex of **5** (0.91 g, 0.81 mmol), triisopropylacetylene (0.37 mL, 2.04 mmol), Pd(PPh₃)₂Cl₂ (0.11 g, 0.16 mmol), CuI (0.047 g, 0.24 mmol), THF (30 mL) and NEt₃ (5 mL) was gently refluxed for 4 h under dinitrogen. The solvent was removed under vacuum. The residue was purified by column chromatography (silica gel) using DCM/hexanes = 1/4 to as eluent to give the product (0.82 g, 83%) as a purple solid. ¹H NMR (CDCl₃, 400 MHz) δ_H 10.21 (s, 1H), 9.91 (d, *J*=4.4 Hz, 2H), 9.38 (d, *J*=4.4 Hz, 2H), 9.11 (d, *J*=4.8 Hz, 2H), 9.09 (d, *J*=4.8 Hz, 2H), 7.79 (t, *J*=8.4 Hz, 2H), 7.11 (d, *J*=8.8 Hz, 4H), 3.95 (t, *J*=6.4 Hz, 8H), 1.68-1.57 (m, 21H), 1.09-1.02 (m, 8H), 0.97-0.86 (m, 8H), 0.71-0.45 (m, 44H). ¹³C NMR (CDCl₃, 100 MHz) δ_C 160.5, 152.6, 151.5, 150.9, 149.7, 132.5, 132.1, 131.9, 131.2, 130.3, 121.8, 114.3, 110.9, 106.9, 105.9, 99.6, 96.5, 69.3, 31.8, 29.1, 29.0, 25.7, 22.7, 19.7, 19.6,

19.2, 19.1, 14.3, 12.5, 12.3, 11.9. FAB-MS: m/z calcd for $C_{75}H_{104}N_4O_4SiZn$ 1218, found 1219 $[M+1]^+$.

[5-Bromo-15-(triisopropylsilyl)ethynyl-10,20-bis(2,6-di-octoxyphenyl)porphyrinato] zinc(II) (7)

To a stirred solution of porphyrin **6** (0.82 g, 0.67 mmol) in DCM (250 mL) and pyridine (10 mL) was added NBS (0.14 g, 0.80 mmol) at 23 °C. After stirring for 0.5 h, the reaction was quenched with acetone (25 mL). The solvent was removed under reduced pressure. The residue was purified by column chromatography (silica gel) using DCM/hexanes = 1/4 to as eluent to give the product (0.74 g, 85%). 1H NMR ($CDCl_3$, 400 MHz) δ_H 9.72 (d, $J=4.8$ Hz, 2H), 9.65 (d, $J=4.8$ Hz, 2H), 8.92 (d, $J=4.8$ Hz, 2H), 8.89 (d, $J=4.8$ Hz, 2H), 7.71 (t, $J=8.0$ Hz, 2H), 7.03 (d, $J=8.4$ Hz, 4H), 3.88 (t, $J=6.4$ Hz, 8H), 1.55-1.45 (m, 21H), 1.02-0.95 (m, 8H), 0.89-0.80 (m, 8H), 0.66-0.39 (m, 44H). ^{13}C NMR ($CDCl_3$, 100 MHz) δ_C 160.4, 153.4, 151.9, 151.1, 149.4, 133.1, 132.9, 132.5, 131.5, 130.4, 121.4, 115.3, 110.4, 105.8, 105.5, 100.0, 97.0, 69.2, 31.8, 31.3, 29.1, 25.7, 22.7, 19.5, 14.3, 12.4, 12.2. FAB-MS: m/z calcd for $C_{75}H_{103}BrN_4O_4SiZn$ 1296, found 1297 $[M+1]^+$.

[5-Bis(4-hexylphenyl)amino-15-(Triisopropylsilyl)ethynyl-10,20-bis(2,6-di-octoxyphenyl)porphyrinato] Zinc(II) (8)

A mixture of bis(4-hexylphenyl)amine (0.34 g, 1.02 mmol), and 60 % NaH (0.04 g, 1.02 mmol), porphyrin **7** (0.33 g, 0.25 mmol), DPEphos (0.05 g, 0.09 mmol) and $Pd(OAc)_2$ (0.014 g, 0.06 mmol) in dry toluene (30 mL) was gently refluxed for 4 h under dinitrogen. The solvent was removed under vacuum. The residue was purified by column chromatography (silica gel) using DCM/hexanes = 1/4 as eluent to give the product (0.33 g, 71%). 1H NMR ($CDCl_3$, 400 MHz) δ_H 9.66 (d, $J=4.4$ Hz, 2H), 9.19 (d, $J=4.4$ Hz, 2H), 8.86 (d, $J=4.4$ Hz, 2H), 8.70 (d, $J=4.8$ Hz, 2H), 7.64 (t, $J=8.4$ Hz, 2H), 7.22 (t, $J=8.8$ Hz, 4H), 6.94 (m, 8H), 3.82 (t, $J=6.4$ Hz, 8H), 2.46 (t, $J=7.6$ Hz, 4H), 1.55-1.52 (m, 4H), 1.49-1.43 (m, 21H), 1.27 (t, 12H), 1.01-0.94 (m, 8H), 0.88-0.76 (m, 22H), 0.65-0.43 (m, 44H). ^{13}C NMR ($CDCl_3$, 100 MHz) δ_C 160.3, 152.9, 152.4, 151.0, 150.6, 135.1, 132.5, 131.0, 130.9, 130.2, 129.1, 123.3, 122.4, 121.4, 114.7, 110.6, 105.7, 99.7, 96.6, 69.1, 35.7, 32.2, 32.0, 31.8, 31.4, 29.6, 29.0, 28.9, 25.6, 23.1, 22.7, 19.6, 19.5, 14.5, 14.2, 14.0, 12.4. FAB-MS: m/z calcd for $C_{99}H_{137}N_5O_4SiZn$ 1553, found 1554 $[M+1]^+$.

[5,15-bis(2,6-dioctoxyphenyl)-10-(bis(4-hexylphenyl)amino)-20-(4-carboxyphenyl)

ethynyl)porphyrinato] Zinc(II) (YD2-*o*-C8)

To a solution of porphyrin **8** (120 mg, 0.077 mmol) in dry THF (10 mL) was added TBAF (0.39 mL, 1M in THF). The solution was stirred at 23 °C for 30 min under dinitrogen. The mixture was quenched with H₂O and then extracted with CH₂Cl₂. The organic layer was dried over anhydrous MgSO₄ and the solvent was removed under reduced pressure. The residue and 4-iodobenzoic acid (93 mg, 0.38 mmol) were dissolved in a mixture of dry THF (18 mL) and NEt₃ (3.5 mL) and the solution was degassed with dinitrogen for 10 min; Pd₂(dba)₃ (21 mg, 0.023 mmol) and AsPh₃ (46 mg, 0.15 mmol) were added to the mixture. The solution was refluxed for 4 h under dinitrogen. The solvent was removed under reduced pressure. The residue was purified by column chromatography (silica gel) using DCM/CH₃OH = 20/1 as eluent. Recrystallization from CH₃OH/Ether to give **YD2-*o*-C8** (88 mg, 77%) as a green solid. ¹H NMR (CDCl₃/d₅-pyridine, 400 MHz) δ_H 9.57 (d, *J*=4.8 Hz, 2H), 9.00 (d, *J*=4.4 Hz, 2H), 8.79 (d, *J*=4.4 Hz, 2H), 8.58 (d, *J*=4.8 Hz, 2H), 8.26 (d, *J*=8.4 Hz, 2H), 7.99 (d, *J*=8.0 Hz, 2H), 7.61 (t, *J*=8.4 Hz, 2H), 6.98 (d, *J*=8.0 Hz, 4H), 6.93 (d, *J*=8.4 Hz, 4H), 6.77 (d, *J*=8.4 Hz, 4H), 3.79 (t, *J*=6.4 Hz, 8H), 2.38 (t, *J*=7.6 Hz, 4H), 1.47 (s, 4H), 1.21 (s, 12H), 0.89 (t, *J*=7.6 Hz, 16H), 0.81-0.72 (m, 14H), 0.62-0.41 (m, 36H). ¹³C NMR (CDCl₃, 100 MHz) δ_C 160.4, 152.5, 152.4, 151.0, 150.8, 135.1, 132.7, 132.5, 132.0, 131.7, 131.0, 130.8, 130.6, 130.4, 130.3, 129.9, 129.2, 123.8, 122.4, 121.4, 115.0, 109.2, 105.7, 98.4, 97.6, 95.1, 69.1, 35.7, 32.2, 31.9, 31.3, 30.2, 30.0, 29.6, 29.1, 28.9, 25.6, 23.1, 22.7, 14.5, 14.3. FAB-MS: *m/z* calcd for C₉₇H₁₂₁N₅O₆Zn 1517, found 1518 [M+1]⁺.

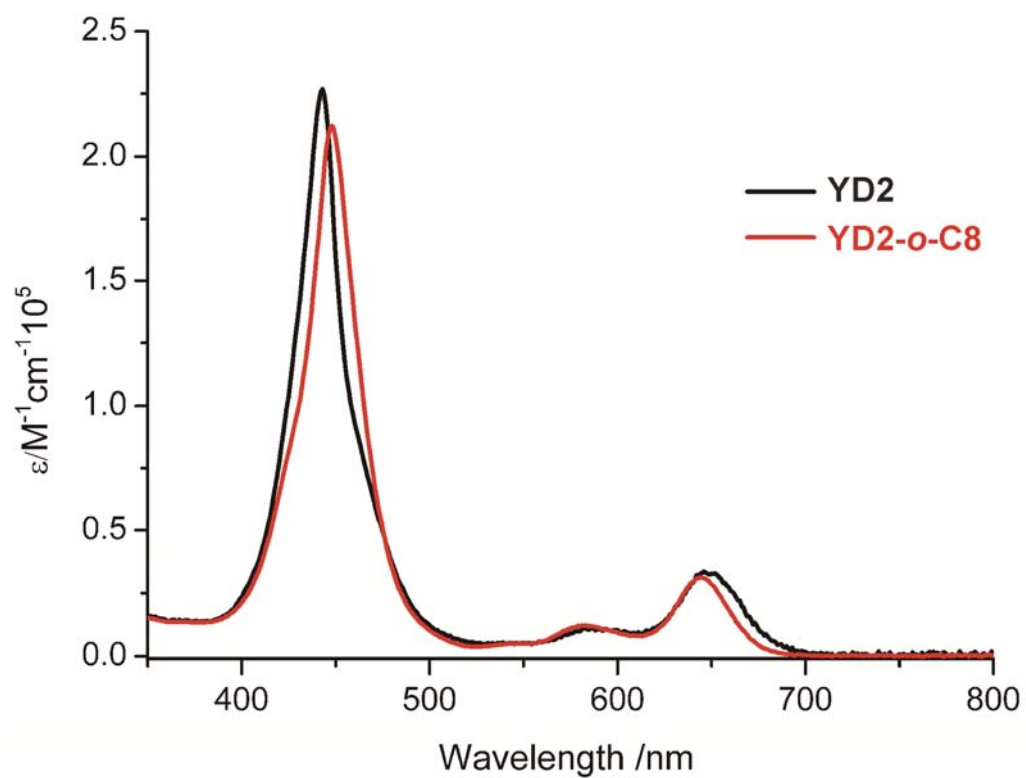


Fig. S1. Absorption spectra of porphyrins **YD2** and **YD2-*o*-C8** in THF.

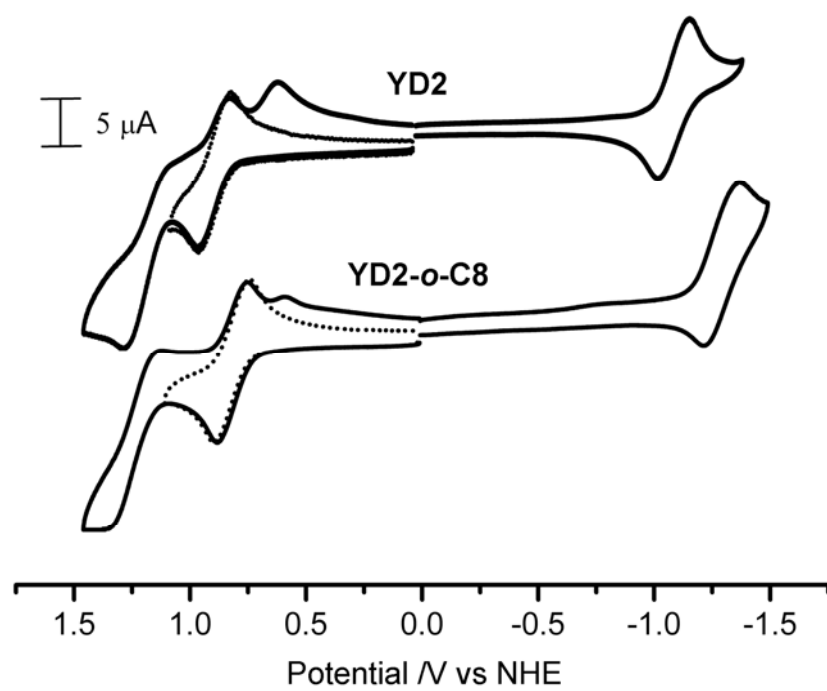


Fig. S2. Cyclic voltammograms of **YD2** and **YD2-*o*-C8** in THF containing TBAPF₆ (0.1 M) at 23 °C.

Table S1 Spectral and electrochemical data for porphyrin dyes.[†]

Dye	Absorption $\lambda_{\text{max}}/\text{nm}$ ($\epsilon/10^3 \text{ M}^{-1} \text{ cm}^{-1}$)	Emission [‡] $\lambda_{\text{max}}/\text{nm}$ (ϕ)	Oxidation $E_{1/2}/\text{V}$	Reduction $E_{1/2}/\text{V}$
YD2	443(227), 586(11), 646(34)	676	+0.89, +1.29 [§]	-1.10
YD2-<i>o</i>-C8	448(212), 581(12), 645(31)	663	+0.82, +1.37 [§]	-1.29

[†] Absorption and emission data were measured in THF at 23 °C. Electrochemical measurements were performed at 23 °C in THF containing TBAPF₆ (0.1 M) as supporting electrolyte. Potentials measured vs. ferrocene/ferrocenium (Fc/Fc⁺) couple were converted to normal hydrogen electrode (NHE) by addition of +0.63 V.

[‡] The excitation wavelengths were 646 and 645 nm for **YD2** and **YD2-*o*-C8**, respectively, in THF.

[§] Irreversible process E_{pa} .

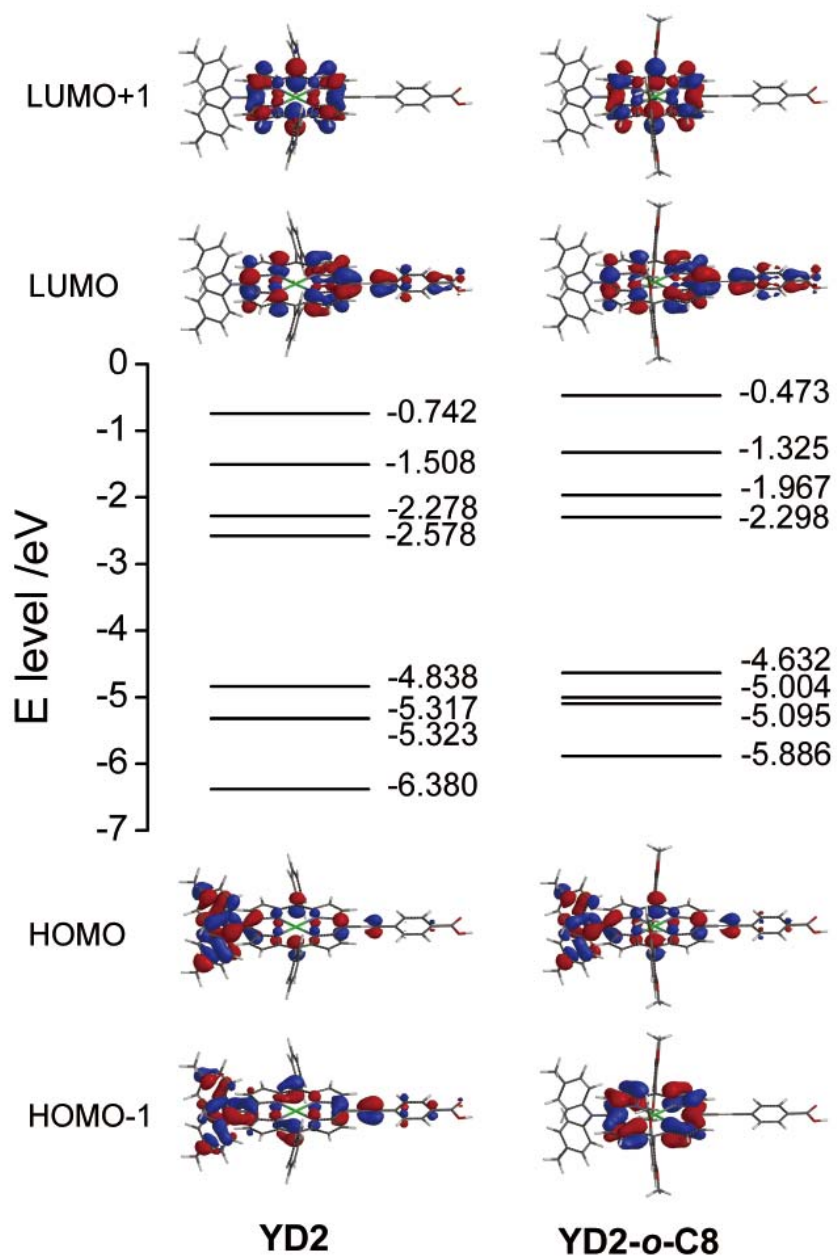


Fig. S3. Energy-level diagram and the corresponding molecular orbitals of porphyrins **YD2** and **YD2-o-C8** calculated by density-functional theory (DFT) at the B3LYP/6-31G(d) level (Spartan 08 package).

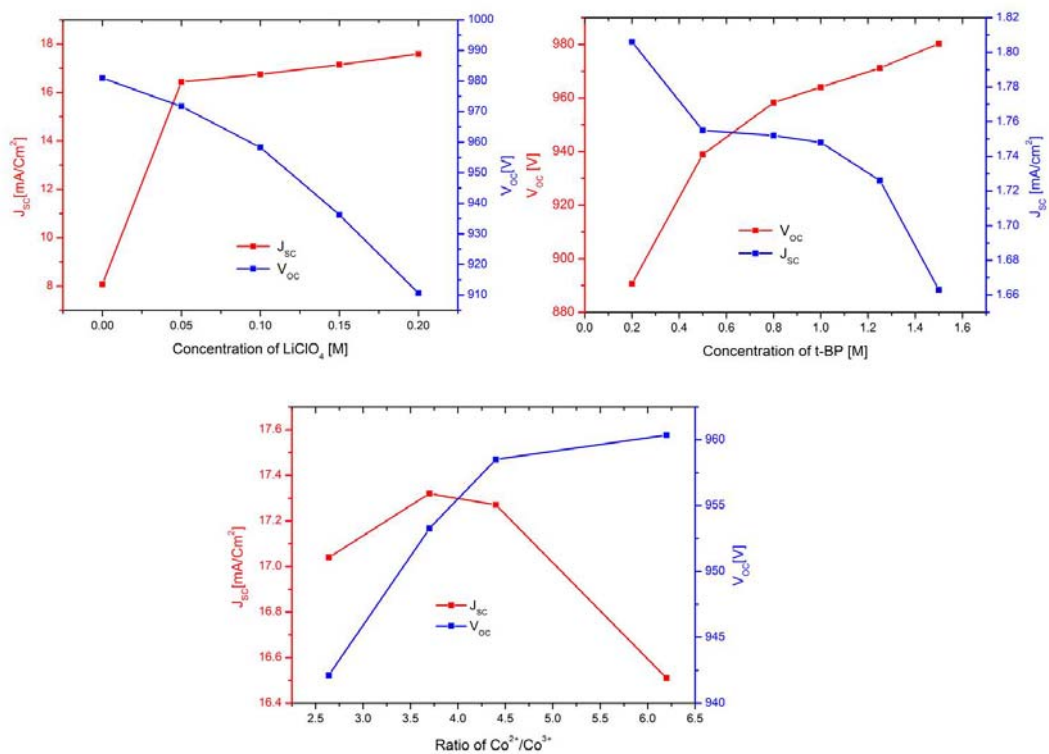


Fig. S4. Optimization of Co^(II/III)tris(bipyridyl)-based electrolytes by varying the concentrations of TBP, lithium ion and ratio of Co⁺²/Co⁺³ in the electrolyte.

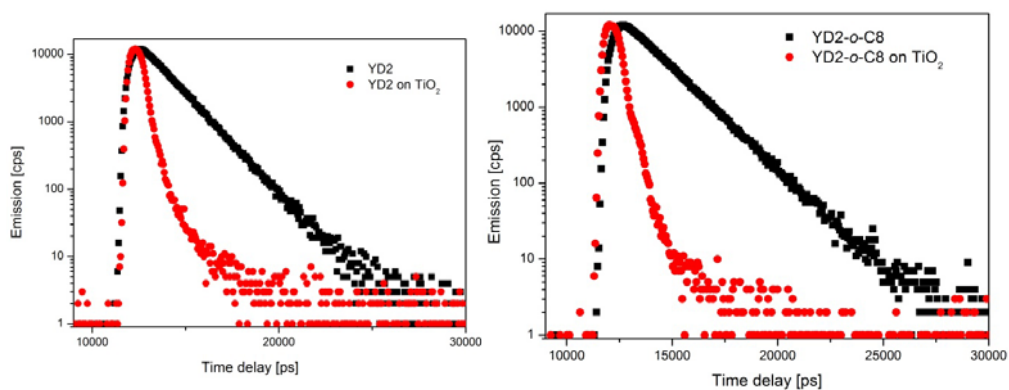


Fig. S5 left : time-resolved luminescence of **YD-o-C8** in THF solution (black points) and adsorbed on a nanocrystalline TiO_2 film in the presence of $\text{Co}^{(\text{II/III})}$ tris(bipyridyl) based redox electrolyte (red points). Right : same measurements and color code for **YD2**.

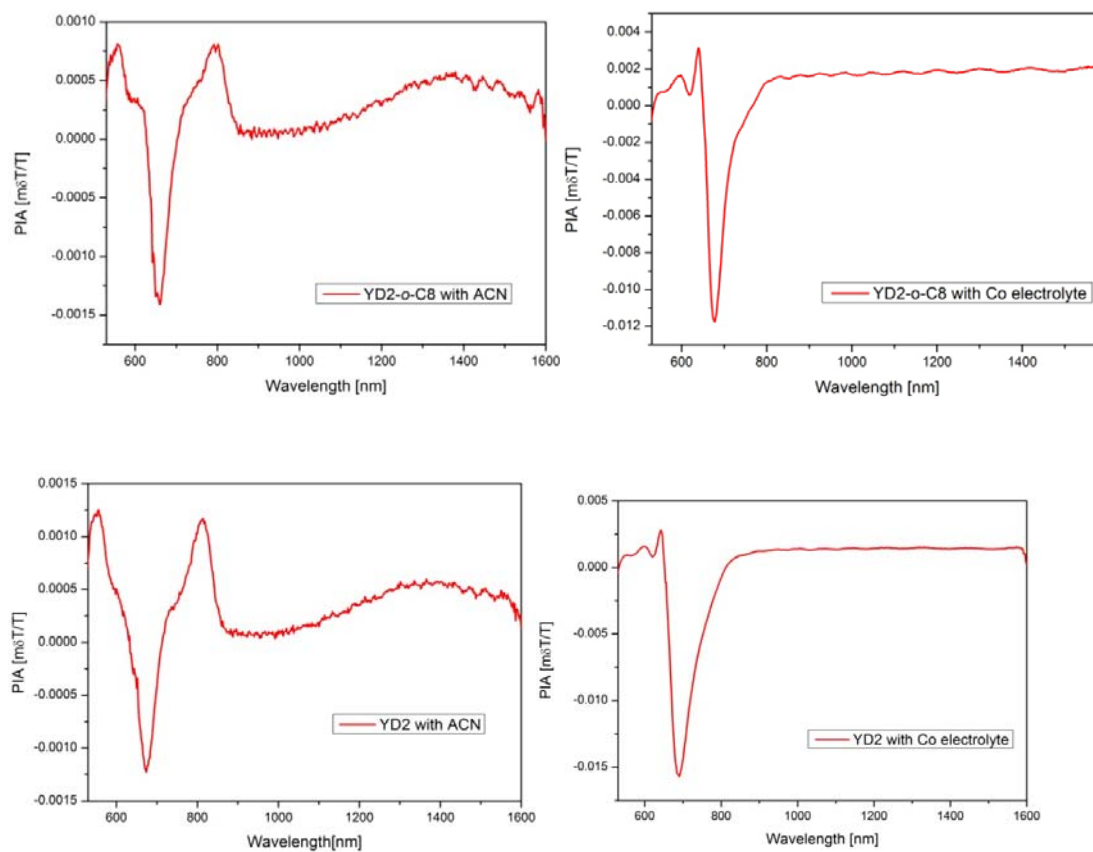


Fig. S6 Photo-induced transient absorption studies carried out with **YD-*o*-C8** and **YD2** sensitized nanocrystalline TiO₂ films in acetonitrile in the absence (top) and presence (bottom) of Co^(II/III)tris(bipyridyl) redox electrolyte.

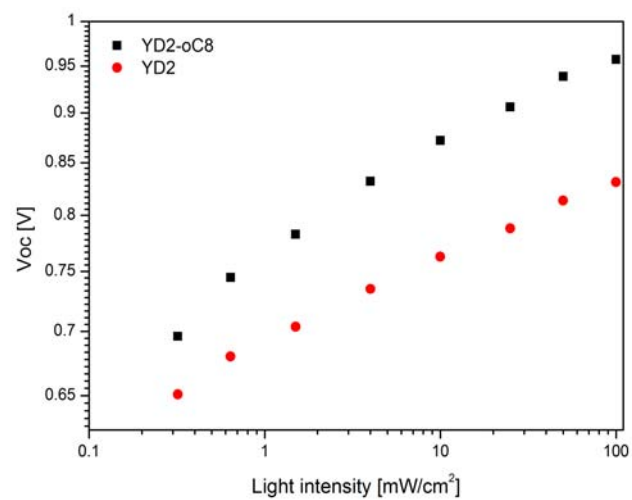


Fig. S7 Dependence of the V_{oc} on light intensity for a DSC with $\text{Co}^{\text{II/III}}$ tris(bipyridyl)-based electrolyte (AY1) with two different dyes **YD2** and **YD2-*o*-C8** porphyrin sensitizers.

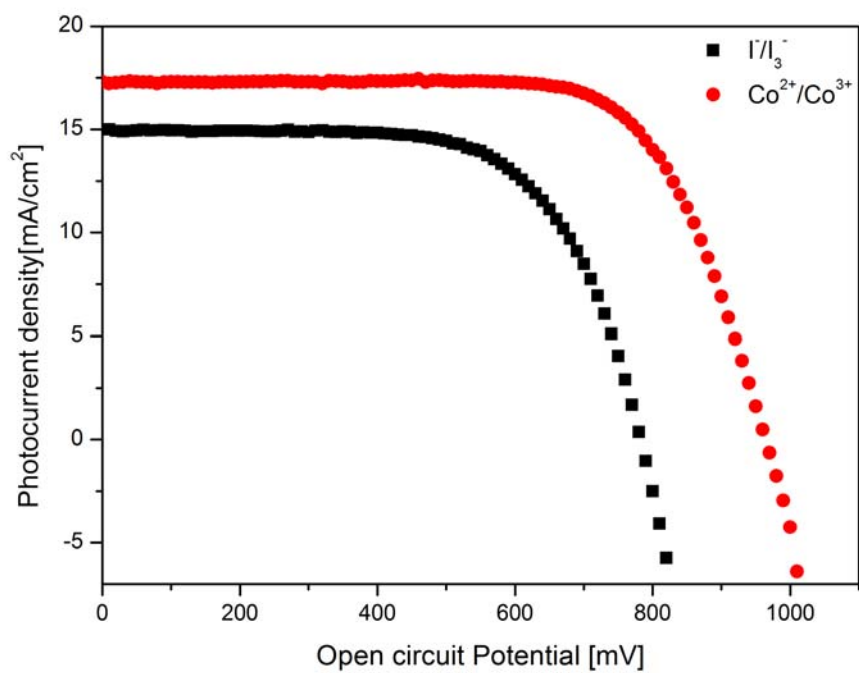


Fig S8. Comparison of the I-V curves with the $\text{Co}^{\text{II/III}}$ tris(bipyridyl) redox couple and I^-/I_3^- redox couple using the same concentration of the redox species.

Table S2 Comparison of photovoltaic parameters of devices made with dye **YD2-o-C8** porphyrin using different redox electrolytes.

Electrolyte	J_{sc} (mA/cm ²)	V_{oc} (mV)	FF	η (%)
AY1	17.3	965	0.71	11.9
AY2	15.0	772	0.66	7.6
Z959	15.8	832	0.71	9.4

AY1 = 0.165M [Co(bpy)₃](B(CN)₄)₂, 0.045M [Co(bpy)₃](B(CN)₄)₃, 0.8M *tert*-butyl pyridine (TBP) and 0.1M LiClO₄ in acetonitrile.

AY2 = 0.165M 1,3-dimethylimidazolium iodide, 0.045M I₂, 0.8M *tert*-butyl pyridine (TBP) and 0.1M LiClO₄ in acetonitrile.

Z959 = (1.0 M 1,3-dimethylimidazolium iodide (DMII), 0.03M iodine, 0.1M guanidinium thiocyanate and 0.5M *tert*-butylpyridine in a mixture of valeronitrile/ acetonitrile (15:85 v/v)).

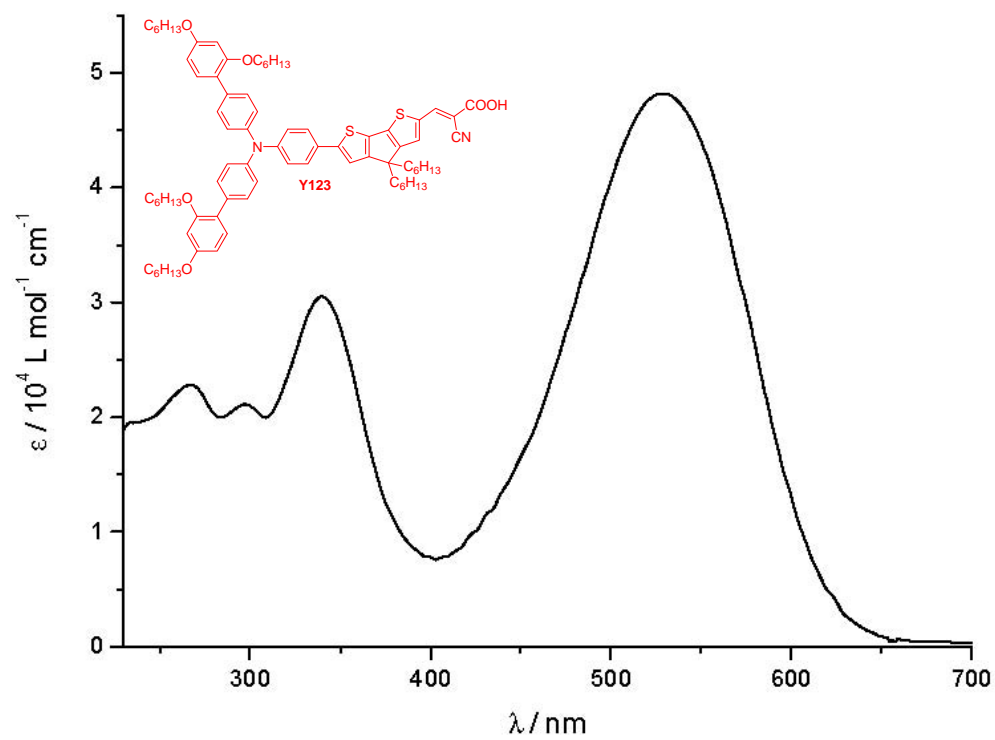


Fig. S9 Absorption spectra of **Y123** dye in THF. Inset shows the molecular structure of this sensitizer.

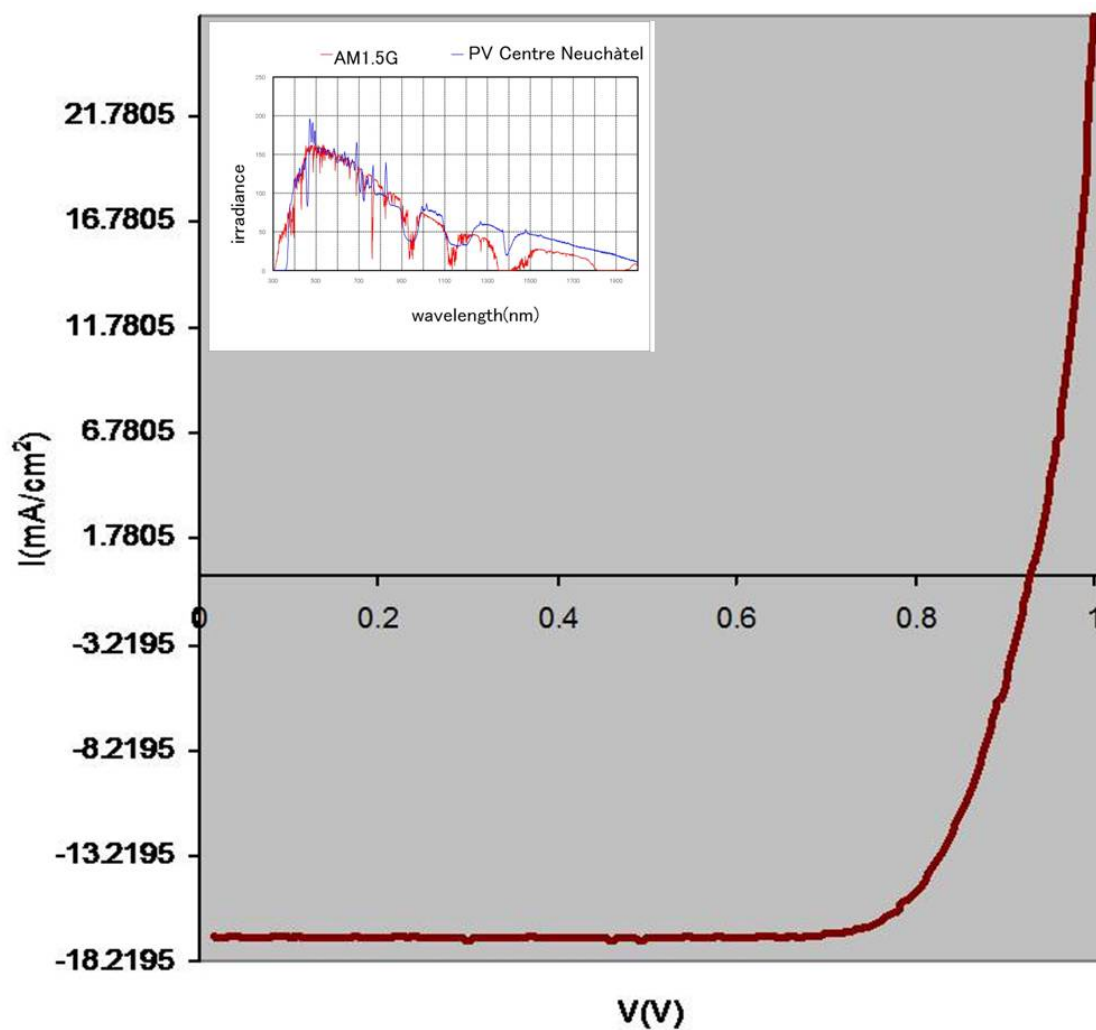


Fig. S10. J-V characteristics of **YD2-*o*-C8/Y123** co-sensitized DSC, measured by the Swiss Photovoltaic Laboratory at the Institute of Micro Technique (IMT) Neuchâtel Switzerland. The lab is operating a large area dc ($2.2 \times 2.2 \text{ cm}^2$), dual lamp, Wacom high precision solar simulator system class AAA mimicking very closely the solar spectrum in the absorption range of the co-sensitized solar cells in the range of 350 to 750 nm. Inset shows the spectral irradiance of the solar simulator employed at the IMT PV lab in comparison to the standard AM 1.5 solar emission spectrum.

Table S3 Photovoltaic performance parameters of a device sensitized by a mixture of **YD2-o-C8** and **Y123** (molar ratio of 4:1 in the staining solution) employing AY1 electrolyte at full sunlight intensity. The cells were measured at the Swiss Photovoltaic Laboratory at the Institute of Micro Technique (IMT) Neuchâtel Switzerland.

P_{in} (mW/cm²)	J_{sc} (mA/cm²)	V_{oc} (V)	FF	η (%)
10.4	1.843	0.843	0.841	13.07
50.1	9.177	0.896	0.798	13.15
99.5	17.053	0.927	0.779	12.29

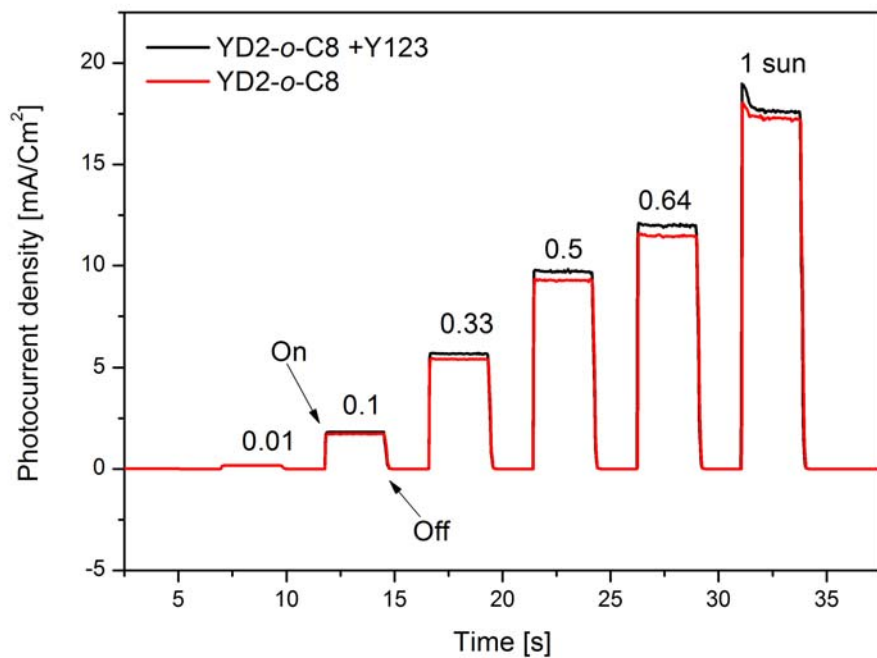


Fig. S11 Photocurrent transient dynamics at different solar intensities. The initial decline of the photocurrent signal at full sun is due to mass transfer limitation.

Table S4 Photovoltaic performance parameters of a device sensitized by a mixture of **YD2-*o*-C8** and **Y123** (molar ratio of 4:1 in the staining solution) employing AY1 electrolyte at different light intensities.

Dye	Electrolyte	P_{in} (mW/cm²)	J_{sc} (mA/cm²)	V_{oc} (mV)	FF	PCE (%)
YD2-<i>o</i>-C8 +Y123	AY1	9.3	1.77	792	0.809	12.2
		51.1	9.57	862	0.773	12.5
		99.7	18.21	891	0.746	12.2

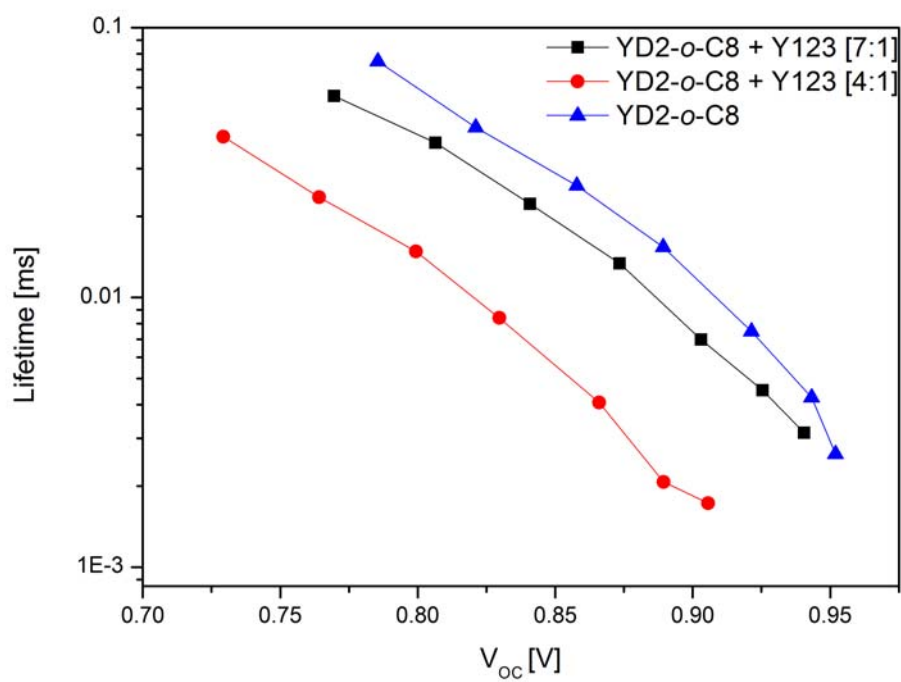


Fig. S12. Electron lifetime determined by photocurrent and photovoltage decay measurements of devices using co-sensitized DSCs with **YD2-o-C8** and **Y123** dyes in different ratios.

References and Notes

1. B. O'Regan, M. Grätzel, A low-cost, high-efficiency solar cell based on dye-sensitized colloidal TiO₂ films. *Nature* **353**, 737 (1991). [doi:10.1038/353737a0](https://doi.org/10.1038/353737a0)
2. Y. Chiba *et al.*, Dye-sensitized solar cells with conversion efficiency of 11.1%. *Jpn. J. Appl. Phys.* **45**, L638 (2006). [doi:10.1143/JJAP.45.L638](https://doi.org/10.1143/JJAP.45.L638)
3. C.-Y. Chen *et al.*, Highly efficient light-harvesting ruthenium sensitizer for thin-film dye-sensitized solar cells. *ACS Nano* **3**, 3103 (2009). [doi:10.1021/nn900756s](https://doi.org/10.1021/nn900756s) [Medline](#)
4. W. Zeng *et al.*, Efficient dye-sensitized solar cells with an organic photosensitizer featuring orderly conjugated ethylenedioxythiophene and dithienosilole blocks. *Chem. Mater.* **22**, 1915 (2010). [doi:10.1021/cm9036988](https://doi.org/10.1021/cm9036988)
5. Q. Yu *et al.*, High-efficiency dye-sensitized solar cells: The influence of lithium ions on exciton dissociation, charge recombination, and surface states. *ACS Nano* **4**, 6032 (2010). [doi:10.1021/nn101384e](https://doi.org/10.1021/nn101384e) [Medline](#)
6. J. M. Kroon *et al.*, Nanocrystalline dye-sensitized solar cells having maximum performance. *Prog. Photovolt. Res. Appl.* **15**, 1 (2007). [doi:10.1002/pip.707](https://doi.org/10.1002/pip.707)
7. M. K. Nazeeruddin *et al.*, Combined experimental and DFT-TDDFT computational study of photoelectrochemical cell ruthenium sensitizers. *J. Am. Chem. Soc.* **127**, 16835 (2005). [doi:10.1021/ja052467l](https://doi.org/10.1021/ja052467l) [Medline](#)
8. Y. Chiba, A. Islam, R. Komiya, N. Koide, L. Y. Han, Conversion efficiency of 10.8% by a dye-sensitized solar cell using a TiO₂ electrode with high haze. *Appl. Phys. Lett.* **88**, 223505 (2006). [doi:10.1063/1.2208920](https://doi.org/10.1063/1.2208920)
9. Z. S. Wang, M. Yanagida, K. Sayama, H. Sugihara, Electronic-insulating coating of CaCO₃ on TiO₂ electrode in dye-sensitized solar cells: Improvement of electron lifetime and efficiency. *Chem. Mater.* **18**, 2912 (2006). [doi:10.1021/cm0603102](https://doi.org/10.1021/cm0603102)
10. M. D. Wei *et al.*, Highly efficient dye-sensitized solar cells composed of mesoporous titanium dioxide. *J. Mater. Chem.* **16**, 1287 (2006). [doi:10.1039/b514647j](https://doi.org/10.1039/b514647j)
11. G. Boschloo, A. Hagfeldt, Characteristics of the iodide/triiodide redox mediator in dye-sensitized solar cells. *Acc. Chem. Res.* **42**, 1819 (2009). [doi:10.1021/ar900138m](https://doi.org/10.1021/ar900138m) [Medline](#)
12. M. Wang, N. Chamberland, L. Breau, J.-E. Moser, R. H.-Baker, B. Marsan, S. M. Zakeeruddin, M. Grätzel. *Nat. Chem.* **2**, 385 (2010). [Medline](#) [doi:10.1038/nchem.610](https://doi.org/10.1038/nchem.610)
13. D. Li *et al.*, Non-Corrosive, Non-absorbing organic redox couple for dye-sensitized solar cells. *Adv. Funct. Mater.* **20**, 3358 (2010). [doi:10.1002/adfm.201000150](https://doi.org/10.1002/adfm.201000150)
14. T. Daeneke *et al.*, High-efficiency dye-sensitized solar cells with ferrocene-based electrolytes. *Nat. Chem.* **3**, 211 (2011). [doi:10.1038/nchem.966](https://doi.org/10.1038/nchem.966) [Medline](#)
15. Y. Bai *et al.*, High-efficiency organic dye-sensitized mesoscopic solar cells with a copper redox shuttle. *Chem. Commun. (Camb.)* **47**, 4376 (2011). [doi:10.1039/c1cc10454c](https://doi.org/10.1039/c1cc10454c) [Medline](#)
16. B. A. Gregg, F. Pichot, S. Ferrere, C. L. Fields, Interfacial recombination processes in dye-sensitized solar cells and methods to passivate the interfaces. *J. Phys. Chem. B* **105**, 1422 (2001). [doi:10.1021/jp003000u](https://doi.org/10.1021/jp003000u)

17. S. Hattori, Y. Wada, S. Yanagida, S. Fukuzumi, Blue copper model complexes with distorted tetragonal geometry acting as effective electron-transfer mediators in dye-sensitized solar cells. *J. Am. Chem. Soc.* **127**, 9648 (2005). [doi:10.1021/ja0506814](https://doi.org/10.1021/ja0506814) [Medline](#)
18. Z. Zhang, P. Chen, T. N. Murakami, S. M. Zakeeruddin, M. Grätzel, The 2,2,6,6-tetramethyl-1-piperidinyloxy radical: An efficient, iodine-free redox mediator for dye-sensitized solar cells. *Adv. Funct. Mater.* **18**, 341 (2008). [doi:10.1002/adfm.200701041](https://doi.org/10.1002/adfm.200701041)
19. H. Nusbaumer, S. M. Zakeeruddin, J. E. Moser, M. Grätzel, An alternative efficient redox couple for the dye-sensitized solar cell system. *Chemistry* **9**, 3756 (2003). [doi:10.1002/chem.200204577](https://doi.org/10.1002/chem.200204577) [Medline](#)
20. S. A. Sapp, C. M. Elliott, C. Contado, S. Caramori, C. A. Bignozzi, Substituted polypyridine complexes of cobalt(II/III) as efficient electron-transfer mediators in dye-sensitized solar cells. *J. Am. Chem. Soc.* **124**, 11215 (2002). [doi:10.1021/ja027355y](https://doi.org/10.1021/ja027355y) [Medline](#)
21. H. Nusbaumer, J. E. Moser, S. M. Zakeeruddin, M. K. Nazeeruddin, M. Grätzel, $\text{Co}^{\text{II}}(\text{dbbip})_2^{2+}$ complex rivals tri-iodide/iodide redox mediator in dye-sensitized photovoltaic cells. *J. Phys. Chem. B* **105**, 10461 (2001). [doi:10.1021/jp012075a](https://doi.org/10.1021/jp012075a)
22. S. M. Feldt *et al.*, Design of organic dyes and cobalt polypyridine redox mediators for high-efficiency dye-sensitized solar cells. *J. Am. Chem. Soc.* **132**, 16714 (2010). [doi:10.1021/ja1088869](https://doi.org/10.1021/ja1088869) [Medline](#)
23. H. N. Tsao *et al.*, Cyclopentadithiophene bridged donor-acceptor dyes achieve high power conversion efficiencies in dye-sensitized solar cells based on the tris-cobalt bipyridine redox couple. *ChemSusChem* **4**, 591 (2011). [doi:10.1002/cssc.201100120](https://doi.org/10.1002/cssc.201100120) [Medline](#)
24. Z. Difei *et al.*, *Energy. Environ. Sci.* **4**, 2030 (2011).
25. J. N. Clifford, G. Yahioğlu, L. R. Milgrom, J. R. Durrant, Molecular control of recombination dynamics in dye sensitised nanocrystalline TiO_2 films. *Chem. Commun. (Camb.)* **12**, 1260 (2002). [doi:10.1039/b201855a](https://doi.org/10.1039/b201855a) [Medline](#)
26. T. Hasobe *et al.*, Photovoltaic cells using composite nanoclusters of porphyrins and fullerenes with gold nanoparticles. *J. Am. Chem. Soc.* **127**, 1216 (2005). [doi:10.1021/ja047768u](https://doi.org/10.1021/ja047768u) [Medline](#)
27. T. Hasobe *et al.*, Enhancement of light-energy conversion efficiency by multi-porphyrin arrays of porphyrin-peptide oligomers with fullerene clusters. *J. Phys. Chem. B* **109**, 19 (2005). [doi:10.1021/jp045246v](https://doi.org/10.1021/jp045246v) [Medline](#)
28. M. Borgström *et al.*, *J. Phys. Chem. B* **109**, 22928 (2005). [Medline](#) [doi:10.1021/jp054034a](https://doi.org/10.1021/jp054034a)
29. C.-W. Lee *et al.*, Novel zinc porphyrin sensitizers for dye-sensitized solar cells: Synthesis and spectral, electrochemical, and photovoltaic properties. *Chemistry* **15**, 1403 (2009). [doi:10.1002/chem.200801572](https://doi.org/10.1002/chem.200801572) [Medline](#)
30. A. Huijser, T. J. Savenije, A. Kotlewski, S. J. Picken, L. D. A. Siebbeles, Efficient light-harvesting layers of homeotropically aligned porphyrin derivatives. *Adv. Mater. (Deerfield Beach Fla.)* **18**, 2234 (2006). [doi:10.1002/adma.200600045](https://doi.org/10.1002/adma.200600045)
31. O. Hagemann, M. Jørgensen, F. C. Krebs, Synthesis of an all-in-one molecule (for organic solar cells). *J. Org. Chem.* **71**, 5546 (2006). [doi:10.1021/jo060491r](https://doi.org/10.1021/jo060491r) [Medline](#)

32. G. M. Hasselman *et al.*, Theoretical solar-to-electrical energy-conversion efficiencies of perylene-porphyrin light-harvesting arrays. *J. Phys. Chem. B* **110**, 25430 (2006). [doi:10.1021/jp064547x](https://doi.org/10.1021/jp064547x) [Medline](#)
33. S. Eu *et al.*, Effects of 5-membered heteroaromatic spacers on structures of porphyrin films and photovoltaic properties of porphyrin-sensitized TiO₂ cells. *J. Phys. Chem. C* **111**, 3528 (2007). [doi:10.1021/jp067290b](https://doi.org/10.1021/jp067290b)
34. T. Bessho, S. M. Zakeeruddin, C. Y. Yeh, E. W. G. Diau, M. Grätzel, Highly efficient mesoscopic dye-sensitized solar cells based on donor-acceptor-substituted porphyrins. *Angew. Chem. Int. Ed.* **49**, 6646 (2010). [doi:10.1002/anie.201002118](https://doi.org/10.1002/anie.201002118)
35. H.-P. Lu *et al.*, Control of Dye Aggregation and electron injection for highly efficient porphyrin sensitizers adsorbed on semiconductor films with varying ratios of coadsorbate. *J. Phys. Chem. C* **113**, 20990 (2009). [doi:10.1021/jp908100v](https://doi.org/10.1021/jp908100v)
36. C.-P. Hsieh *et al.*, Synthesis and characterization of porphyrin sensitizers with various electron-donating substituents for highly efficient dye-sensitized solar cells. *J. Mater. Chem.* **20**, 1127 (2010). [doi:10.1039/b919645e](https://doi.org/10.1039/b919645e)
37. S.-L. Wu *et al.*, Energy. *Environ. Sci.* **3**, 949 (2010).
38. J.-C. Chang, C.-J. Ma, G.-H. Lee, S.-M. Peng, C.-Y. Yeh, Porphyrin-triarylamine conjugates: strong electronic communication between triarylamine redox centers via the porphyrin dication. *Dalton Trans.* **8**, 1504 (2005). [doi:10.1039/b417350c](https://doi.org/10.1039/b417350c) [Medline](#)
39. H.-P. Lu *et al.*, Design and characterization of highly efficient porphyrin sensitizers for green see-through dye-sensitized solar cells. *Phys. Chem. Chem. Phys.* **11**, 10270 (2009). [doi:10.1039/b917271h](https://doi.org/10.1039/b917271h) [Medline](#)
40. C.-L. Mai *et al.*, Synthesis and characterization of diporphyrin sensitizers for dye-sensitized solar cells. *Chem. Commun. (Camb.)* **46**, 809 (2010). [doi:10.1039/b917316a](https://doi.org/10.1039/b917316a) [Medline](#)
41. H. J. Snaith *et al.*, Charge collection and pore filling in solid-state dye-sensitized solar cells. *Nanotechnology* **19**, 424003 (2008). [doi:10.1088/0957-4484/19/42/424003](https://doi.org/10.1088/0957-4484/19/42/424003) [Medline](#)
42. B. C. O'Regan, F. J. Lenzmann, Charge transport and recombination in a nanoscale interpenetrating network of n-type and p-type semiconductors: Transient photocurrent and photovoltage studies of TiO₂/dye/CuSCN photovoltaic cells. *J. Phys. Chem. B* **108**, 4342 (2004). [doi:10.1021/jp035613n](https://doi.org/10.1021/jp035613n)
43. K. O'Regan, Bakker, J. Kroeze, H. Smit, P. Sommeling, James R. Durrant. *J. Phys. Chem. B* **110**, 17155 (2006). [Medline](#) [doi:10.1021/jp062761f](https://doi.org/10.1021/jp062761f)
44. P. Siders, R. A. Marcus, Quantum effects in electron-transfer reactions. *J. Am. Chem. Soc.* **103**, 741 (1981). [doi:10.1021/ja00394a003](https://doi.org/10.1021/ja00394a003)
45. J. N. Clifford, E. Martínez-Ferrero, A. Viterisi, E. Palomares, Sensitizer molecular structure-device efficiency relationship in dye sensitized solar cells. *Chem. Soc. Rev.* **40**, 1635 (2011). [doi:10.1039/b920664g](https://doi.org/10.1039/b920664g) [Medline](#)
46. J. J. Nelson, T. J. Amick, C. M. Elliott, Mass transport of polypyridyl cobalt complexes in dye-sensitized solar cells with mesoporous TiO₂ photoanodes. *J. Phys. Chem. C* **112**, 18255 (2008). [doi:10.1021/jp806479k](https://doi.org/10.1021/jp806479k)

47. B. Mohr, V. Enkelmann, G. Wegner, Synthesis of alkyl- and alkoxy-substituted benzils and oxidative coupling to tetraalkoxyphenanthrene-9,10-diones. *J. Org. Chem.* **59**, 635 (1994). [doi:10.1021/jo00082a022](https://doi.org/10.1021/jo00082a022)
48. K. E. Splan, J. T. Hupp, Permeable nonaggregating porphyrin thin films that display enhanced photophysical properties. *Langmuir* **20**, 10560 (2004). [doi:10.1021/la048465g](https://doi.org/10.1021/la048465g) [Medline](#)

Acknowledgements: E.W.-G.D. and C.Y.Y. acknowledge the financial support from the National Science Council of Taiwan and Ministry of Education of Taiwan. M.G. thanks the European Research Council (ERC) for an Advanced Research Grant (ARG 247404) funded under the “Mesolight” project. Financial support under the European community’s 7th FWP for project 227057 (INNOVASOL) and under a grant from the Dayton U.S. Air force Research Laboratory is gratefully acknowledged. M.K.N. thanks World Class University program, Photovoltaic Materials, Department of Material Chemistry, Korea University, Chungnam 339-700, Korea, which is funded by the Ministry of Education, Science and Technology through the National Research Foundation of Korea (R31-2008-000-10035-0). We thank R. Humphry-Baker for fruitful discussions as well as optical measurements and M. J. M. Bonnet-Eymard from the IMT Photovoltaic Laboratory for assistance with the cell photovoltaic performance measurements.